Applied Surface Science 457 (2018) 655–661

Contents lists available at ScienceDirect

Applied Surface Science

journal homepage: www.elsevier.com/locate/apsusc

Full Length Article

Facile synthesis of carbon-supported silver nanoparticles for optical limiting

Huanhuan Xu, Lihe Yan*, Yang Yu, Yanmin Xu

Key Laboratory for Physical Electronics and Devices of the Ministry of Education & Shaanxi Key Lab of Information Photonic Technique, School of Electronics & Information Engineering, Xi'an Jiaotong University, Xi'an 710049, China

ARTICLE INFO

Keywords:
Carbon nanodots
Carbon supported silver nanoparticles
Optical limiting

ABSTRACT

Photoexcited carbon nanodots (CDs) could be both excellent electron donors and electron acceptors, offering potential applications in photochemical reactions. Using the CDs as the reductant, carbon-supported silver nanoparticles (Ag-CDs) are synthesized by ultraviolet light irradiation. The influence of the surface chemical structure of the CDs, irradiation light wavelength, reaction time, and reactant concentration on the reaction products are systematically studied. Using a nanosecond laser, we investigate the nonlinear optical response of the as-prepared Ag-CDs, which show excellent optical limiting (OL) behaviors. The OL threshold of Ag-CDs is estimated to be 0.6 J/cm^2, which is much lower than that of CDs with the OL threshold of 2.2 J/cm^2. The OL mechanism of the material is mainly attributed to the enhanced nonlinear scattering effect induced by the synergistic effect of the silver nanoparticles (Ag NPs) and supporting CDs.

1. Introduction

With their rapid development, high power laser sources have been used in many fields including industry, military, medicine, etc [1,2]. The increasing usage of laser sources triggers a great challenge to design efficient optical limiting (OL) materials and devices to protect human eyes and delicate detecting devices from optical damage [3–8]. Nonlinear OL processes, such as nonlinear scattering (NLS), nonlinear absorption (NLA), refractive index change, have been studied in various materials [9]. Many organic and inorganic materials have been proved to be good candidates for optical limiters, among which carbon-based materials, such as fullerenes [10], carbon black suspensions (CBS) [11], carbon nanotubes (CNTs) [12], carbon nanodots (CDs) [13,14], and grapheme [15–17] have exhibited excellent OL performance.

As a typical noble metal material with nanometer size, silver nanoparticles (Ag NPs) have also attracted a great deal of attentions in nonlinear optical areas due to their discrete energy levels and confined electrons of atoms [18–21]. In general, chemical reduction is the most frequently used method for the preparation of Ag NPs as stable, colloidal dispersions in water or organic solvents. Ag NPs were synthesized by reducing silver ions with reductants such as borohydride, hydrazine, citrate, and elemental hydrogen [22–24]. However, the use of surfactants might introduce impurities and impede their applications, and the reducing reagents might cause environmental toxicity or biological hazards [25–27]. Besides, the previous studies have shown that the size, morphology, stability and properties (chemical and physical) of the Ag NPs are strongly influenced by the experimental conditions, the kinetics of interaction of metal ions with reducing agents, and adsorption processes of stabilizing agent with metal nanoparticles [28]. Hence, green and simple synthetic methods would be desirable. As has been summarized by V. K. Sharma, the green synthetic methods include mixed-valence polyoxometallates, polysaccharide, Tollens, irradiation, and biological strategies, while the synthesis of Ag NPs involves the selection of solvent medium, environmentally benign reducing agent, and nontoxic substances for stability [29].

As a novel carbon-based nanomaterial with sizes below 10 nm, carbon nanodots (CDs) have found many applications in many areas such as biosensing and bioimaging, drug transfer, and optoelectronic devices. Since they were firstly discovered in 2004 by purifying single-walled carbon nanotubes through preparative electrophoresis, significant research efforts have been expended to produce CDs with controlled dimensions and surface properties, using many techniques including combustion, laser ablation, microwave processing, silica template methods and so on [30–36]. Among these synthetic strategies, laser synthesis and processing of colloids (LSPC) can provide a green, simple and scalable method to synthesis CDs, and also plays an important role in synthesis of surfactant-free metal or metal oxides NPs [36]. Because the carbon surfaces exist generous functional groups (hydroxyl, carbonyl, carboxyl and epoxy groups), photoexcited CDs have been proved to be both excellent electron acceptors and electron donors [37]. Based on their excellent electron-donating capability, Ag NPs were firstly synthesized using CDs as the reductant and supporting material by UV light irradiation in 2013 [38]. This synthesis strategy provides a fast, simple and clean method (tens of minutes' exposure to a

* Corresponding author.
E-mail address: liheyan@mail.xjtu.edu.cn (L. Yan).

https://doi.org/10.1016/j.apsusc.2018.07.006
Received 17 January 2018; Received in revised form 10 June 2018; Accepted 2 July 2018
Available online 03 July 2018
0169-4332/

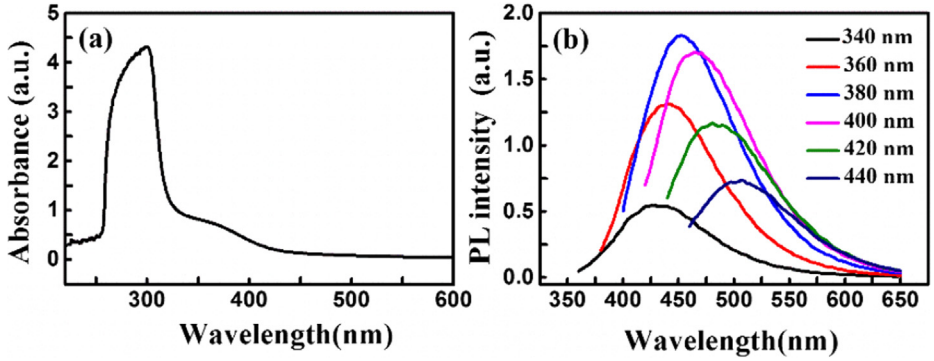

Fig. 1. (a) UV–Vis spectrum of CDs, (b) Fluorescence spectra of CDs.

UV lamp) to prepare Ag-CDs NPs. Besides, as there are abundant hydrophilic groups on the CDs such as –OH, the prepared Ag-CDs NPs can be monodispersed in solvents, and the dispersions in solvents possess well stability even without any substances.

Although many researches have been focused on the synthesis and biological and optoelectronic applications of the Ag-CDs, little attention has been devoted to the nonlinear optical properties of the Ag-CDs. Besides that, the controllability of UV light assisted synthesis of Ag-CDs materials is still needed to be studied in depth. In this study, CDs prepared using femtosecond laser ablation method are used to synthesize Ag NPs by UV light irradiation. The influence of reaction conditions such as the surface chemical structure of the CDs, irradiation light wavelength, reaction time, and Ag ion concentration on the reaction products are studied. The OL behaviors of the as-prepared Ag-CDs are studied using a nanosecond laser Z-scan technique. The results indicate that Ag-CDs have a lower OL threshold than C_{60}, and the OL mechanism is mainly due to the enhanced nonlinear scattering effect induced by the synergistic effect of the Ag NPs and supporting CDs.

2. Experimental

2.1. Chemicals

Polyethylene glycol (PEG_{200}) and N-Methyl pyrrolidone (NMP) were purchased from Sinopharm Chemical Reagent Co., Ltd. Graphite powder was purchased from Aladdin Chemistry Co., Ltd (China).

2.2. Synthesis of CDs

The CDs were synthesized by femtosecond laser ablation of graphite powders in different liquids (distilled water, PEG_{200}, and NMP) at room temperature. In a typical procedure, 0.1 mg of graphite powder with a mean size of 400 nm was dispersed into 50 ml of solvent. Then 10 ml of suspension was put into a glass beaker for laser ablation. A Ti: sapphire femtosecond laser system with central wavelength of 800 nm, pulse duration of 100 fs and repetition rate of 1 kHz was used. The laser beam was focused into the suspension by a 100 mm lens for 0.5 h. During the laser ablation, a magnetic stirrer was used to prevent the suspended powders from gravitational settling in the solvent. After laser ablation, large graphite particles were removed by centrifuging the dispersion at 10000 rpm for 10 min.

2.3. Synthesis of Ag-CDs nanoparticles

Silver nitrate with different concentrations was dispersed into 10 ml of as-prepared CDs liquid, and then the mixed solution was put into a glass beaker for UV irradiation with different wavelength. Due to the generous functional groups of the carbon surfaces, the electron transfer from the photoexcited CDs can reduce the Ag ions to Ag NPs on their surface. During this procedure, the mixed solution changes from yellow to dark brown, indicating the conversion of Ag^+ ions to Ag NPs [38].

2.4. OL measurements of Ag-CDs

The OL behaviors of Ag-CDs solutions were studied using 10 ns laser pulses emitted from a Q-switched Nd^{3+}: YAG laser. The laser was operated at the second harmonic of 532 nm with a pulse repetition rate of 10 Hz. The laser source was focused with an f = 20 cm lens. An open-aperture (OA) and closed-aperture (CA) Z-scan system is used to measure the OL behavior of the dispersions [15]. As a reference, OL behavior of the C_{60} solution in toluene was also measured. All the dispersions were filled in a 2 mm thick quartz cells, and the linear transmittances of all the samples were adjusted to 80% by changing the solute concentrations.

To clarify the OL mechanisms of the samples, we measured the pulse energy dependence of the scattered light intensity for the samples. A fraction of the scattered light was collected using a convex lens at ~30° in the forward direction from the beam axis, and then detected by a photodiode. To investigate the contribution of nonlinear absorption (NLA) effect on the OL property of the samples, a part of the output

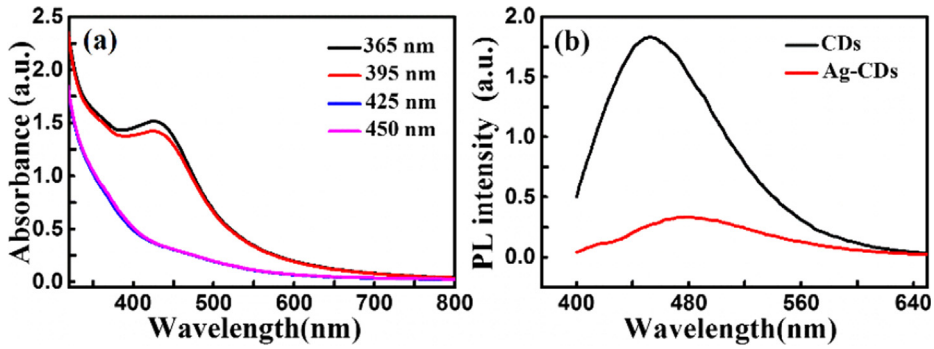

Fig. 2. (a) UV–Vis spectra of Ag-CDs synthetized with different UV light wavelength, (b) PL spectra of CDs and Ag-CDs at 380 nm excitation.

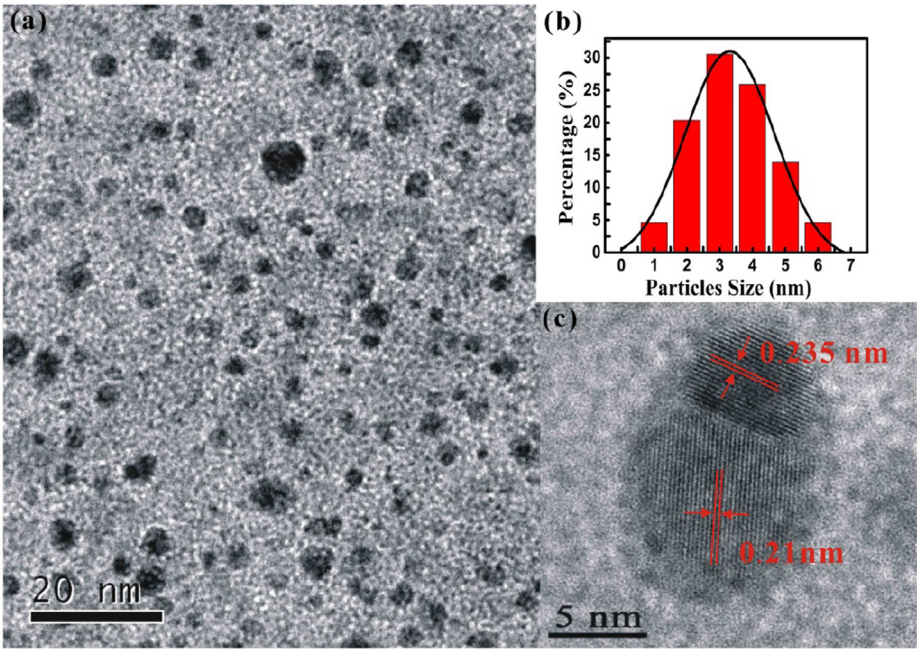

Fig. 3. (a) TEM images of the as prepared Ag-CDs, (b) the corresponding size distributions of the Ag-CDs, and (c) the HRTEM images of the Ag-CDs.

beam from the sample including amounts of scattered light is collected by a lens and detected by the detector. By measuring the incident power dependence of the nonlinear transmittance of the samples, the contributions of the NLA effect to OL behaviors can be confirmed.

3. Results and discussion

3.1. Characterizations of CDs

Firstly, the optical properties of the CDs prepared using femtosecond laser ablation method in NMP were characterized using UV–Vis and PL spectroscopies. Fig. 1(a) shows that absorption spectrum of the CDs, which has an obvious optical absorption peak at 298 nm and a small absorption peak at 380 nm with an edge extending to around 420 nm. The peak at 298 nm is typically ascribed to $n \rightarrow \pi^*$ of C = O, while the absorption edge extending to 420 nm can be attributed to electron transition of $n \rightarrow \pi^*$ for C = N [39]. These strong absorption peaks indicate the abundant surface functionalization groups on the carbon core. From the PL spectra in Fig. 1(b), the CDs show strong fluorescence emissions by excitation from 340 nm to 440 nm. The strongest fluorescence emission centered at around 450 nm is observed at when excited by 380 nm excitation. As has been demonstrated in our previous study, the intense PL in CDs is originated mainly from the abundant functional groups on their surface [40–42]. The photoexcited CDs can act as excellent electron donors and provide potential applications in photochemical reactions [37].

Fig. 2(a) shows the absorption spectra of CDs synthetized in NMP mixed with silver nitrate after irradiation under light with different wavelength. The mean size of the CD is about 2.3 nm (as shown in Fig. S1(c)) and Ag ions concentration is 2.5×10^{-2} mM. The as-prepared Ag-CDs are synthesized by ultraviolet light irradiation for 15 min. It can be seen from the figure that the absorption spectra of the solution irradiated by 365 nm and 395 nm light have an obvious peak at around 420 nm, which could be attributed to the surface plasmon resonance (SPR) absorption of the Ag NPs. As comparisons, no characteristic absorption peak of Ag-NPs is observed when the solution is irradiated by 425 nm and 450 nm light. Fig. 2(b) shows the PL spectra of CDs without (black line) and with (red line) Ag NPs under 380 nm excitation. With the presence of Ag NPs, the photo-induced electrons will probably transfer to the metal, and nonradiative recombination takes place, causing the decrease the PL intensity of CDs.

Supplementary data associated with this article can be found, in the online version, at https://doi.org/10.1016/j.apsusc.2018.07.006.

The formation mechanism of Ag NPs can be attributed to the electron transfer between the photoexcited CDs and the Ag^+ ions. Ag ions are attracted to the surface of CDs via electrostatic interactions with some functional groups. After irradiation, free electrons from the photoexcited CDs reach the Ag^+ ions at the surface, and the interfacial junction allows more electrons to pass through to the conductive Ag nucleation site and to reduce more Ag^+ ions, eventually forming Ag-CD NPs [38]. The reduction of Ag^+ ions is highly dependent on the amount of the electron-hole pairs generated in the photo-excitation process, and dependent on the PL intensity of the CDs to a certain extent. According to Fig. 2(a), Ag^+ ions can be reduced at the excitation of 365 nm and 395 nm, but cannot be reduced at 425 nm excitation, even though the PL intensity is considerable strong at 420 nm excitation (as shown in Fig. 1(a)). We speculate that the different electron excitation and recombination paths are responsible to the reducibility of the CDs excited by different wavelength light. As has been demonstrated in our previous report [43], both the intrinsic states of carbonic core and the surface states might be excited when the CDs are excited by short wavelength light, while only surface states could be excited under long wavelength light. As has been reported by Y. Choi et al, excited electrons are more likely transfer from the carbonic core to the Ag nucleus in its growth progress [44]. On these bases, we infer that when the CDs are excited by 365 nm and 395 nm, electrons are easily excited into the intrinsic states of carbonic core and then transfer to Ag^+ ions, resulting in the formation of Ag NPs and the quenching of the PL intensity. However, when the CDs are excited by 425 nm and 450 nm light, electrons are excited into the surface states and then relax to the ground state of the CDs through radiative recombination. To verify our speculation, the PL intensity of the Ag-CDs under different excitations is studied. As shown by Fig. S2, the quenching effect of Ag NPs decreases with increasing the excitation wavelength, indicating that electrons are more likely to transfer to the Ag NPs under short wavelength excitation. When the CDs are excited by long wavelength light, excited electrons are generated on the functional groups, and most of them are relaxed into the ground states through radiative recombination rather than transferring to the Ag NPs through interfacial junction between the carbonic core and Ag NPs.

The morphology and structure of as-prepared Ag-CDs nanoparticles are characterized by TEM and HRTEM images. The mean size of the CD synthetized in NMP is about 2.3 nm and Ag ions concentration is 1×10^{-1} mM. The as-prepared Ag-CDs are synthesized by ultraviolet light irradiation for 15 min. As shown by the TEM image in Fig. 3(a), the as-prepared Ag-CDs nanoparticles distribute on the copper grid homogeneously, and no large aggregations are observed, indicating that the Ag-CDs nanoparticles are well dispersed in the solution. Fig. 3(b) shows the size distributions of the Ag-CDs nanoparticles, in which the sample showed a size distribution from 0.5 nm to 6.5 nm with the mean size of about 3.86 nm. The HRTEM image is given in Fig. 3(c). From the figure we can see that there are two different lattice spacing stripes, the lattice spacing distance of the narrow stripes is 0.21 nm, which was in close match with the (1 0 0) lattice spacing of graphite carbon [39]. Another lattice spacing distance is 0.235 nm, which correspond to (2 0 0) crystallographic planes of Ag [45]. This indicates that Ag NPs are formed adjacent the CDs. The contact of the Ag NPs and CDs might change the dynamics of photo-excited carriers, and thereby the PL as well as other optical properties [46].

3.2. The effect of experimental parameters on synthetic Ag-CDs nanoparticles

In order to control the optical properties of the Ag-CDs nanoparticles, we investigated the effect of experimental parameters on the preparation of Ag-CDs nanoparticles. Firstly, we prepared CDs with different PL properties by changing the solvent used in the ablation process. Fig. 4(a) shows the PL of the CDs synthetized in distilled water (black line), PEG (red line), NMP (blue line), respectively. The CDs in different solvents show different PL properties, which is mainly due to the different surface functional groups [40]. Generally speaking, the CDs in NMP show the strongest PL intensity, while the fluorescence of those in distilled water is very weak. Fig. 4(b) is the absorption spectra of the Ag-CDs nanoparticles prepared by CDs synthetized in different solvents. Obviously, the CDs synthesized in distilled water does not reduce Ag ions to Ag NPs whereas the CDs synthesized in PEG can reduce Ag ions to silver nanoparticles even though the absorption peak of silver is weak. By comparison, the absorption peak of Ag NPs reduced by CDs in NMP solution is the strongest under the same reaction conditions.

To obtain insights into the difference of the reducibility of CDs prepared in different solvents, the morphologies and chemical structures of the CDs are studied using TEM imaging, FTIR and XPS spectrometry, respectively. As indicated by the TEM images (Fig. S1), the mean size of particle sizes of the CD synthetized in three solvents differs very little. Hence, we infer that the reducibility of CDs is correlated to the functional groups on the surface of CDs. The FTIR spectra of the CDs prepared using different solvents are given in Fig. 4(c). There are stretching and bending vibrations of CH_2 and CH_3 at around 2920, 2850 cm^{-1} and 1460, 1384 cm^{-1}. The absorption bands at 1544 cm^{-1} and 1634 cm^{-1} correspond to the stretching vibrations of C = C and C = O [41]. The samples prepared in PEG and NMP contain more functional groups than that prepared in water. Besides, the stretching vibrations of N-H at 3360 cm^{-1} appear only in the CDs synthetized in the NMP, meaning that the CDs synthetized in NMP contain nitrogen-containing groups [42]. Fig. 4(d) is the XPS full scan spectra of the Ag-CDs nanoparticles synthetized in different solvents. Consistent with the analysis of FTIR spectrum, the XPS full scan also confirm that the amino groups appear only in the CDs synthetized in the NMP. The high resolution C1s, O1s and N1s spectra also confirm that CDs synthetized in NMP contain more functional groups (see Figs. S3–S5 in the Supporting Information). According to the previous reports, the PL of CDs prepared using laser ablation methods originates mainly from the surface states formed by the surface functional groups. When the CDs are excited by UV light, electron-hole pairs are generated and their radiative recombination will cause the strong luminance [40]. On the other hand, the photo-generated electrons can act as excellent reductant with the presence of Ag ions, causing the formation of the Ag NPs [37]. As the CDs prepared in NMP contain more functional groups, the PL is stronger than those prepared in PEG and distilled water (as shown in Fig. 4(a)). Meanwhile, the strong reducibility of the CDs in NMP will induce the formation of more Ag NPs after UV light irradiation, exhibiting a strong absorption peak at 420 nm (as shown in Fig. 4(b)).

Secondly, we studied the effects of UV light irradiation time and Ag ions concentration on the Ag-CDs. Fig. 5(a) and (b) show the absorption spectra of the Ag-CDs nanoparticles synthesized with different

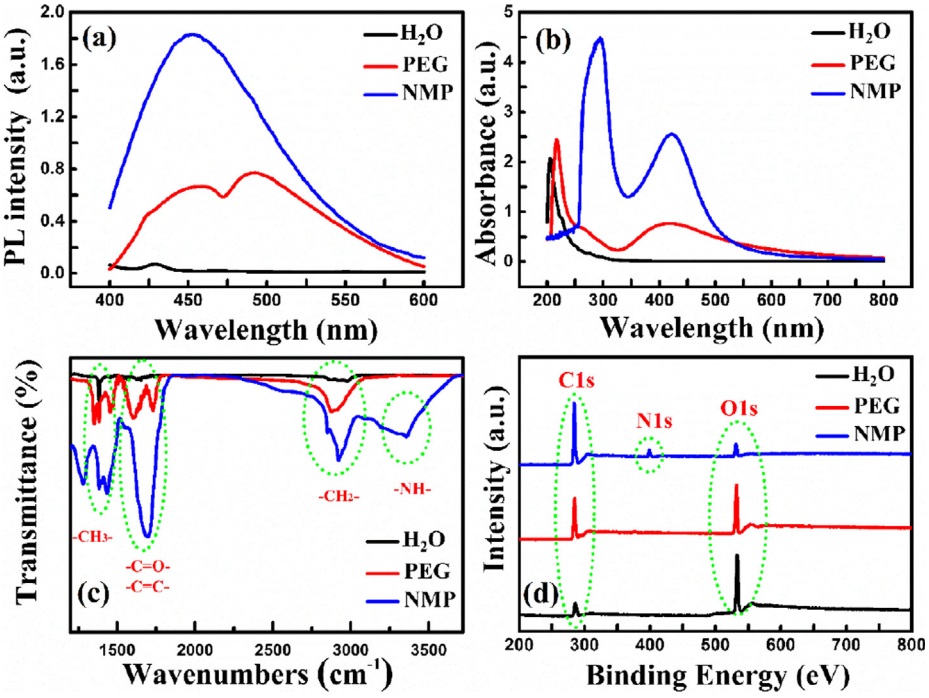

Fig. 4. (a) Fluorescence spectra of CDs, (b) UV–Vis, (c) FTIR and (d) XPS spectra of Ag-CDs synthetized in distilled water, PEG, and NMP.

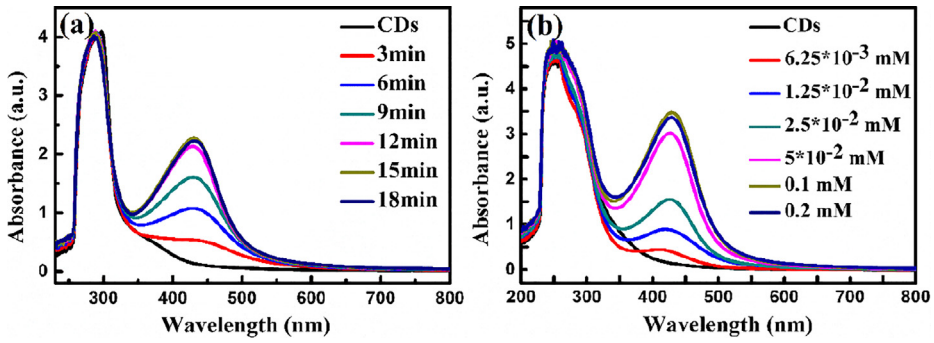

Fig. 5. UV–Vis spectra of Ag-CDs prepared under different (a) illumination time, and (b) silver nitrate concentration.

irradiation time and Ag ions concentrations respectively. As shown by Fig. 5(a), the absorption peak of Ag NPs increases with time, but saturated when the irradiation time increases to more than 15 min. The absorption peak of Ag NPs also increases with increasing the concentration of Ag ions, and saturated when the concentration increases to be more than 1×10^{-1} mM. The enhancement of the absorption around 420 nm is ascribed to the increase of the Ag NPs by increasing the irradiation time and Ag ions concentration. However, the exhaustion of photoexcited CDs will stop the further reduction of Ag ions when the reaction time is further prolonged as well as the ions concentration is further increased. In fact, longer UV light irradiation time and higher Ag ions concentration might cause the aggregation of Ag NPs, and slight precipitation can be found on the wall of the reaction vessel when the reaction time is longer than 15 min or the concentration is beyond 0.1 mM. TEM images of the Ag-CDs are also presented to study the influence of Ag ions concentration on the particle size and morphology. The results indicate that the products keep being well monodispersed, and the mean size of particles changed little with varying the Ag ions concentrations (as shown in Fig. S6).

3.3. OL properties of the Ag-CDs

In some previous reports, the nonlinear optical response of Ag NPs has been studied due to their discrete energy levels and confined electrons of atoms [5,11]. Here, we investigate the nonlinear OL properties of Ag-CDs using the nanosecond and femtosecond laser Z-scan technique. Ag-CDs synthesized under different Ag ions concentrations are measured in our experiments. As a comparison, the OL behavior of C_{60} solution in toluene is also measured under the same experimental conditions.

Fig. 6(a) shows the nonlinear transmittance of the Ag-CDs and C_{60} solution as functions of the distance between the sample and the laser focus. From the figure, we can see that the optical transmittance of Ag-CDs solutions decreased sharply when the sample moves close to the focus, showing obvious OL behaviors. The OL performance is enhanced when the concentration Ag ions increases from 0 to 0.1 mM, indicating that Ag NPs play an important role in the OL process. By comparing with the OL property of C_{60}, the OL threshold (input pulse energy density when the nonlinear transmittance decreases to 50%) is much lower for the Ag-CDs with high concentration. The lowest OL threshold is estimated to be about 0.6 J/cm^2 (Ag ions concentration of 1×10^{-4} M), while the OL threshold of the CDs is estimated to be about

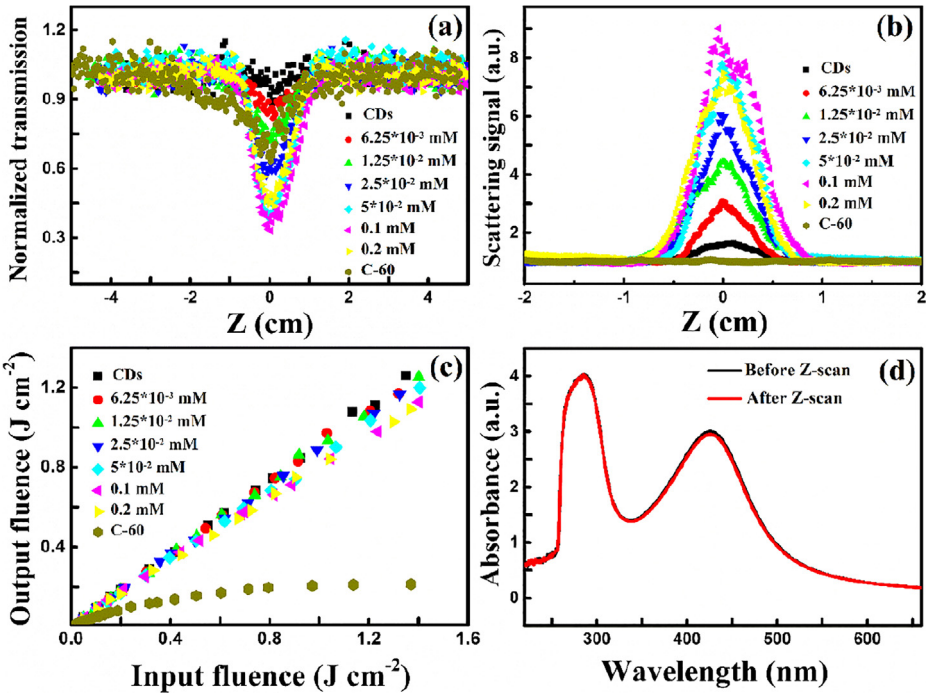

Fig. 6. (a) OL and (b) nonlinear scatting signals and (c) the output fluence as a function of the input fluence of Ag-CDs and C_{60}, (d) the absorption spectrum of the Ag-CDs before and after the Z-scan.

2.2 J/cm^2. The OL performance of the Ag-CDs is comparable with the Ag NPs reported in some previous reports [20,21,47].

Fig. 6(b) shows the nonlinear scattered light intensity as a function of the incident light intensity. As has been demonstrated in the previous reports, little scattered light is detected in C_{60} solution as the OL behavior of the sample was mainly originated from nonlinear absorption effect [48,49]. For Ag-CDs solutions, the onset of the growth of scattered signals is synchronous with the onset of the decrease of transmission for solutions, indicating NLS effect contribute a lot to the OL process of the Ag-CDs. For suspensions of light absorbing carbonic particles, nonlinear scattering effect has been demonstrated to be responsible to the OL behavior of the material [50–52]. When particles were heated by the intense light, they would transfer thermal energy to the surrounding solvents, which would be evaporated and result in the formation of gas bubbles. When the gas bubble becomes large enough, they will scatter and attenuate the incident light. In our experiments, since the absorption edge of the SPR peak of Ag NPs supported on the CDs can extend to 532 nm, the absorption of the incident laser pulse is slightly enhanced by the addition of Ag NPs. With increasing the concentration of the Ag-CDs, the amount of scattering gas bubbles increases and the NLS effect is enhanced, and as the result the OL performance of the composites could be strengthened. Using the numerical modeling provided by K. Metwally, the fluence threshold for the photothermal bubble generation in our experiments is calculated to be 0.36 J/cm^2 [53]. This value accorded well with the measured OL threshold of 0.6 J/cm^2. As the NLS effect takes place when the bubbles are large enough, it's reasonable that the OL threshold should be larger than the threshold for the bubble formation.

Meanwhile, the contribution of NLA effect to the OL behavior is also investigated by collecting the nonlinear scattered light. Fig. 6(c) shows the output fluence of the samples as a function of the input fluence. With the increase of input intensity, the transmittance of the Ag-CDs samples keeps almost constant. As comparison, the transmittance of C_{60} sample decreases obviously with increasing the incident laser intensity. These results indicate that NLA effect contribute little to the OL process of the Ag-CDs samples. Therefore, the OL process of the Ag-CDs sample originated mainly from the nonlinear scattering effect. To study the influence of the laser irradiation on the optical properties of the samples, absorption spectra of the Ag-CDs before and after the Z-scan measurements are measured, and the results indicate that the sample shows well photostability. Besides, successive Z-scan measurements are conducted with the same sample. The OL behavior changed slightly after prolonged and focused nanosecond laser irradiation (as shown by Fig. S7).

Furthermore, closed-aperture Z-scan measurements are performed using the nanosecond pulse laser to study the nonlinear refraction effect of the samples. As the NLS effect is very strong, the influence of nonlinear refractive effect on the closed-aperture Z-scan curve was not able to be extracted (as shown in Fig. S8). As a result, the expected peak-valley curve was not obtained in the nanosecond Z-scan measurements. To eliminate the influence of the nonlinear scattering effect, femtosecond Z-scan measurements are used to study the nonlinear response of the samples. In the femtosecond regime, both saturable absorption (SA) and reversed saturable absorption (RSA) are observed in Ag-CDs samples, while only reversed saturable absorption (RSA) is observed in CDs sample (see Fig. S9 in the Supporting Information). The saturation absorption intensity I_s of the Ag-CDs are determined to be 0.22 MW/cm^2, while the RSA coefficient β_{RSA} values are determined to be 0.42×10^{-10} m/W and 0.26×10^{-10} m/W for CDs and Ag-CDs, respectively. The nonlinear refractive coefficient γ values were determined to be 6.06×10^{-18} m/W, 7.75×10^{-18} m/W for CDs and Ag-CDs, respectively.

4. Conclusions

In conclusion, we propose a fast, simple and green synthesis method of Ag-CDs NPs using CDs as the reducing agent with the assist of UV light irradiation. Due to the hydrophilic property of the CDs, the prepared NPs can be monodispersed in solvents, and the dispersions in solvents possess well stability even without any substances. The influence of the irradiation light wavelength, reaction time, and reactant concentration, especially the PL property of the CDs, on the optical properties of the Ag-CDs NPs are systematically studied. The insight into the PL intensity dependence of the reducibility of the CDs under irradiation with different wavelength indicates that the excitation-recombination pathways paly important roles in the reduction process of Ag ions. Using a nanosecond laser, we investigated the nonlinear optical response of the as-prepared Ag-CDs and found it have excellent OL behaviors. The results indicate that Ag-CDs have a low OL threshold, and the OL mechanism is mainly due to the enhanced nonlinear scattering effect induced by the synergistic effect of the Ag NPs and supporting CDs.

Acknowledgements

This work was supported by National R&D Program of China (2017YFA0207400), and the National Natural Science Foundation of China (Grant No. 61427816, 11674260 and 11474078), the Fundamental Research Funds for the Central Universities, and the collaborative Innovation Center of Suzhou Nano Science and Technology. The TEM work was performed at the International Center for Dielectric Research (ICDR), Xi'an Jiaotong University, Xi'an, China. The authors also thank Mr. Ma and Ms. Lu for their help in using TEM.

References

[1] J. Si, K. Hirao, Phase-matched second-harmonic generation in cross-linking polyurethane films by thermal-assisted optical poling, Appl. Phys. Lett. 91 (2007) 091105.
[2] W. Cui, J. Si, T. Chen, et al., Compact bending sensor based on a fiber Bragg grating in an abrupt biconical taper, Opt. Express 23 (2015) 11031–11036.
[3] P.C. Haripadmam, M.K. Kavitha, H. John, et al., Optical limiting studies of ZnO nanotops and its polymer nanocomposite films, Appl. Phys. Lett. 101 (2012) 071103.
[4] J. Yang, Y. Song, W. Zhu, et al., Investigation of optical nonlinearities and transient dynamics in a stilbenzene derivative, J. Phys. Chem. B. 116 (2012) 1221–1225.
[5] Y. Gao, Y. Wang, Y. Song, et al., Strong optical limiting property of a novel silver nanoparticle containing C60 derivative, Opt. Commun. 223 (2003) 103–108.
[6] S. Bai, Z. Yuan, F. Gao, Colloidal metal halide perovskite nanocrystals: synthesis, characterization, and applications, J. Mater. Chem. C. 4 (2016) 3898–3904.
[7] Z. Gu, D. Li, C. Zheng, Y. Kang, et al., MOF-Templated Synthesis of Ultrasmall Photoluminescent Carbon-Nanodot Arrays for Optical Applications, Angew. Chem. Int. Ed. 56 (2017) 6853–6858.
[8] Z. Gu, J. Zhang, Epitaxial growth and applications of oriented metal–organic framework thin films, Coord. Chem. Rev. (2017), http://dx.doi.org/10.1016/j.ccr.2017.09.028.
[9] N. Venkatram, D.N. Rao, M.A. Akundi, Nonlinear absorption, scattering and optical limiting studies of CdS nanoparticles, Opt. Express 13 (2005) 867–872.
[10] Y.P. Sun, J.E. Riggs, Organic and inorganic optical limiting materials. From fullerenes to nanoparticles, Int. Rev. Phys. Chem. 18 (1999) 43–90.
[11] K. Mansour, M.J. Soileau, E.W. Van Stryland, Nonlinear optical properties of carbon-black suspensions (ink), J. Opt. Soc. Am. B. 9 (1992) 1100–1109.
[12] L. Vivien, P. Lancon, D. Riehl, et al., Carbon nanotubes for optical limiting, Carbon 40 (2002) 1789–1797.
[13] P. Aloukos, I. Papagiannouli, A.B. Bourlinos, et al., Third-order nonlinear optical response and optical limiting of colloidal carbon dots, Opt. Express 22 (2014) 12013.
[14] D. Tan, Y. Yamada, S. Zhou, et al., Carbon nanodots with strong nonlinear optical response, Carbon 69 (2014) 638–640.
[15] L. Yan, Y. Xiong, J. Si, et al., Optical limiting properties and mechanisms of single-layer graphene dispersions in heavy-atom solvents, Opt. Express 22 (2014) 31836–31841.
[16] J. Wang, Yenny Hernandez, Mustafa Lotya, et al., Broadband nonlinear optical response of graphene dispersions, Adv. Mater. 21 (2009) 2430–2435.
[17] X. Cheng, N.N. Dong, B. Li, et al., Controllable broadband nonlinear optical response of graphene dispersions by tuning vacuum pressure, Opt. Express 21 (2013) 16486–16493.
[18] M. Liu, W. Chen, Green synthesis of silver nanoclusters supported on carbon nanodots: enhanced photoluminescence and high catalytic activity for oxygen reduction reaction, Nanoscale 5 (2013) 12558–12564.
[19] C.C. Huang, H.Y. Liao, Y.C. Shiang, et al., Synthesis of wavelength-tunable luminescent gold and gold/silver nanodots, J. Mater. Chem. 19 (2009) 755–759.

[20] R. Sathyavathi, M.B. Krishna, S.V. Rao, et al., Biosynthesis of silver nanoparticles using Coriandrum sativum leaf extract and their application in nonlinear optics, Adv. Sci. Lett. 3 (2010) 138–143.
[21] S. Porel, S. Singh, S.S. Harsha, et al., Nanoparticle-embedded polymer. In situ synthesis, free-standing films with highly monodisperse silver nanoparticles and optical limiting, Chem. Mater. 17 (2005) 9–12.
[22] A.R. Tao, S. Habas, P. Yang, Shape control of colloidal metal nanocrystals, Small 4 (2008) 310–325.
[23] P.C. Lee, D. Meisel, Adsorption and surface-enhanced Raman of dyes on silver and gold sols, J. Phys. Chem 86 (17) (1982) 3391–3395.
[24] K.S. Chou, K.C. Huang, H.H. Lee, Fabrication and sintering effect on the morphologies and conductivity of nano-Ag particle films by the spin coating method, Nanotechnology 16 (2005) 779.
[25] Y. Fang, E. Wang, Simple and direct synthesis of oxygenous carbon supported palladium nanoparticles with high catalytic activity, Nanoscale 5 (2013) 1843–1848.
[26] M.W. Meyer, E.A. Smith, Optimization of silver nanoparticles for surface enhanced Raman spectroscopy of structurally diverse analytes using visible and near-infrared excitation, Analyst 136 (2011) 3542–3549.
[27] J. He, T. Kunitake, Preparation and thermal stability of gold nanoparticles in silk-templated porous filaments of titania and zirconia, Chem. Mater. 16 (2004) 2656–2661.
[28] S. Sengupta, D. Eavarone, I. Capila, et al., Temporal targeting of tumour cells and neovasculature with a nanoscale delivery system, Nature 436 (2005) 568.
[29] V.K. Sharma, R.A. Yngard, Y. Lin, Silver nanoparticles: green synthesis and their antimicrobial activities, Adv. Colloid Interface Sci. 145 (2009) 83–96.
[30] H. Liu, T. Ye, C. Mao, Fluorescent carbon nanoparticles derived from candle soot, Angew. Chem. Int. Ed. 46 (2007) 6473–6475.
[31] V. Nguyen, L. Yan, J. Si, et al., Femtosecond laser-induced size reduction of carbon nanodots in solution: effect of laser fluence, spot size, and irradiation time, J. Appl. Phys. 117 (2015) 084304.
[32] C.M. Luk, L.B. Tang, W.F. Zhang, et al., An efficient and stable fluorescent graphene quantum dot–agar composite as a converting material in white light emitting diodes, J. Mater. Chem. 22 (2012) 22378–22381.
[33] D. Tan, S. Zhou, J. Qiu, et al., Preparation of functional nanomaterials with femtosecond laser ablation in solution, J. Photochem. Photobiol., C 17 (2013) 50–68.
[34] Akansh Nema, R. Pareek, T. Rai, et al., The Role of Glutathione and Ethanol in Dictating the Emission Dynamics of Natural Resources-Derived Highly Luminescent Carbon Nanodots, Chem. Sel. 2 (2017) 11255–11264.
[35] A. Panniello, A.E. Di Mauro, E. Fanizza, et al., Luminescent Oil Soluble Carbon Dots Towards White Light Emission: A Spectroscopic Study, J. Phys. Chem. C. 122 (2018) 839–849.
[36] D. Zhang, B. Gökce, S. Barcikowski, Laser synthesis and processing of colloids: fundamentals and applications, Chem. Rev. 117 (2017) 3990–4103.
[37] X. Wang, L. Cao, F. Lu, et al., Photoinduced electron transfers with carbon dots, Chem. Commun. 25 (2009) 3774–3776.
[38] H. Choi, S.J. Ko, Y. Choi, et al., Versatile surface plasmon resonance of carbon-dot-supported silver nanoparticles in polymer optoelectronic devices, Nat. Photonics 7 (2013) 732–738.
[39] H. Nie, M. Li, Q. Li, et al., Carbon dots with continuously tunable full-color emission and their application in ratiometric pH sensing, Chem. Mater. 26 (2014) 3104–3112.
[40] V. Nguyen, J. Si, L. Yan, et al., Direct demonstration of photoluminescence originated from surface functional groups in carbon nanodots, Carbon 108 (2016) 268–273.
[41] V. Nguyen, L. Yan, H. Xu, One-step synthesis of multi-emission carbon nanodots for ratiometric temperature sensing, Appl. Surf. Sci. 427 (2018) 1118–1123.
[42] Xu. Huanhuan, V. Nguyen, L. Yan, et al., One-step synthesis of nitrogen-doped carbon nanodots for ratiometric pH sensing by femtosecond laser ablation method, Appl. Surf. Sci. 414 (2017) 238–243.
[43] V. Nguyen, J. Si, L. Yan, et al., Electron–hole recombination dynamics in carbon nanodots, Carbon 95 (2015) 659–663.
[44] Y. Choi, G.H. Ryu, S.H. Min, et al., Interface-controlled synthesis of heterodimeric silver–carbon nanoparticles derived from polysaccharides, ACS Nano 8 (2014) 11377–11385.
[45] Y. Zhang, C. Xing, D. Jiang, et al., Facile synthesis of core–shell–satellite Ag/C/Ag nanocomposites using carbon nanodots as reductant and their SERS properties, CrystEngComm 15 (2013) 6305–6310.
[46] H. Zhang, H. Huang, H. Ming, et al., Carbon quantum dots/Ag_3PO_4 complex photocatalysts with enhanced photocatalytic activity and stability under visible light, J. Mater. Chem. 22 (2012) 10501.
[47] Y.P. Sun, J.E. Riggs, H.W. Rollins, et al., Strong optical limiting of silver-containing nanocrystalline particles in stable suspensions, J. Phys. Chem. B. 103 (1999) 77–82.
[48] Lee W. Tutt, Alan Kost, Optical limiting performance of C_{60} and C_{70} solutions, Nature 356 (1992) 225.
[49] R.V. Bensasson, E. Bienvenue, M. Dellinger, et al., C_{60} in model biological systems. A visible-UV absorption study of solvent-dependent parameters and solute aggregation, J. Phys. Chem. 98 (1994) 3492–3500.
[50] Danilo Dini, Mário J.F. Calvete, Michael Hanack, Nonlinear optical materials for the smart filtering of optical radiation, Chem. Rev. 116 (2016) 13043–13233.
[51] Yaobing Xiong, L. Yan, J. Si, et al., Cascaded optical limiter with low activating and high damage thresholds using single-layer graphene and single-walled carbon nanotubes, J. Appl. Phys. 115 (2014) 083111.
[52] Y. Chen, T. Bai, N. Dong, et al., Graphene and its derivatives for laser protection, Prog. Mater. Sci. 84 (2016) 118–157.
[53] Khaled Metwally, Serge Mensah, Guillaume Baffou, Fluence threshold for photothermal bubble generation using plasmonic nanoparticles, J. Phys. Chem. C. 119 (2015) 28586–28596.